Materials Transactions, Vol. 52, No. 3 (2011) pp. 474 to 480
©2011 The Japan Institute of Metals

High Chromium Fe-Cr-Mo-P-C Amorphous Coating Films Produced by Thermal Spraying Technique

Masahiro Komaki[1], Tsunehiro Mimura[1], Ryurou Kurahasi[1], Masahisa Kouzaki[2] and Tohru Yamasaki[3]

[1]*Nakayama Steel Works, Ltd., R&D Division, Osaka 551-8551, Japan*
[2]*Nakayama Steel Works, Ltd., Osaka 551-8551, Japan*
[3]*University of Hyogo, Himeji 671-2280, Japan*

High chromium Fe-Cr-Mo-P-C amorphous coating films containing up to about 35 at% Cr having high hardness and high corrosion resistance have been produced by a newly developed thermal spraying technique. In order to control the temperatures of the powder particles in the flame spray and the substrate, a cylindrical nozzle, with external cooling nitrogen gas, was mounted to the front end of the thermal spraying gun. $Fe_{70}Cr_{10}P_{13}C_7$ and $Fe_{38}Cr_{35}Mo_7P_{13}C_7$ films with various external cooling gas velocities between 20 m/s and 40 m/s exhibited entire amorphous structure without oxides and/or unmelted powder particles. High corrosion-resistance of the $Fe_{38}Cr_{35}Mo_7P_{13}C_7$ amorphous coating film was observed in immersion tests using 35% hydrochloric acid. [doi:10.2320/matertrans.MBW201009]

(Received October 22, 2010; Accepted December 20, 2010; Published February 25, 2011)

Keywords: *high chromium alloys, iron-chromium-molybdenum-phosphorus-carbon, amorphous coating film, thermal spraying method, rapid cooling, hardness, corrosion resistance*

1. Introduction

Thermal spraying method is one of potential candidates to produce amorphous alloy coating films having some excellent properties such as high corrosion resistance and high hardness on large area metallic substrates. Because of the cheaper method compared to other conventional ones such as the vacuum evaporation method, the amorphous alloy coating films by the thermal spraying method can be applied to the wide range of industrial applications.[1–4)]

High chromium Fe-Cr based amorphous alloys containing about 35 at% Cr have excellent high hardness and high corrosion resistance,[5–8)] however, the alloys exhibit the high melting temperatures of about 1000°C and above. Consequently, the high chromium Fe-Cr-based amorphous alloys have not yet been well produced by previous thermal spraying methods. The important problems in these methods may be due to the contamination of oxides and the density of pores in the thermal sprayed films.[1,2,9–13)] Recently, there are some research papers that were able to inhibit the oxide formation by the shield nozzle installed at the front end of the atmospheric plasma spray gun or the high velocity oxygen fuel gun.[14,15)]

In our previous study, we have developed the $Fe_{70}Cr_{10}P_{13}C_7$ amorphous coating films produced by our developed thermal spraying gun with the cylindrical nozzle. The cylindrical nozzle with external cooling nitrogen gas was mounted to the front end of the thermal spray gun to control the temperatures of the powder particles in the flame spray and the substrate. The $Fe_{70}Cr_{10}P_{13}C_7$ spraying films with various external cooling gas velocities between 20 m/s and 40 m/s exhibited an entirely amorphous structure without oxides and/or unmelted powder particles. Corrosion testing has clarified that the sprayed amorphous films exhibited a high corrosion resistance equal to that of Hastelloy C and commercially produced pure titanium. In the immersion conditions of 35% hydrochloric acid, however, the severe corrosion weight loss of the alloy was observed. So the corrosion resistance of the $Fe_{70}Cr_{10}P_{13}C_7$ amorphous coating film did not enough for the practical applications such as the shaft sleeve of the slurry pump.[16)]

In the present study, high chromium Fe-Cr-Mo-P-C amorphous coating films containing up to about 35 at% Cr having excellent high hardness and high corrosion resistance have been produced by the thermal spraying technique with the cylindrical nozzle on shaft sleeve shaped cylindrical SUS304 substrates without cracking and peeling conditions. Corrosion tests of the sprayed films were also done under the severe immersion conditions of 35% hydrochloric acid.

2. Experimental Procedures

The thermal spraying equipment used in this study was composed of a gas flame spraying gun and the cylindrical nozzle. The thermal spraying materials were gas-atomized powders (grain size: 38–63 μm) of $Fe_{70}Cr_{10}P_{13}C_7$ (Fe-10Cr) and $Fe_{38}Cr_{35}Mo_7P_{13}C_7$ (Fe-35Cr) with melting temperatures of 997°C and 1068°C, respectively. A SUS304 (ϕ45 mm × 150 mm × 3 mm) cylindrical substrate, shot blasted by alumina powder, was used. Structural analysis of the coating films was done by X-ray diffraction (Cu-Kα radiation with a graphite monochromator, 40 kV–200 mA) and transmission electron microscopy (TEM:JEM2100-200kV). The amorphous alloy coating films, separated from the substrate, were immersed in 35% hydrochloric acid at room temperature for the maximum period of about 24 h. For comparison, Fe-based amorphous ribbons produced by the single roller type melt spinning apparatus were also immersed in the same corrosion conditions.

Figure 1 shows a schematic illustration of the cylindrical-nozzle type thermal spray gun and the cylindrical substrate that is rotating during the spraying. Table 1 also shows the

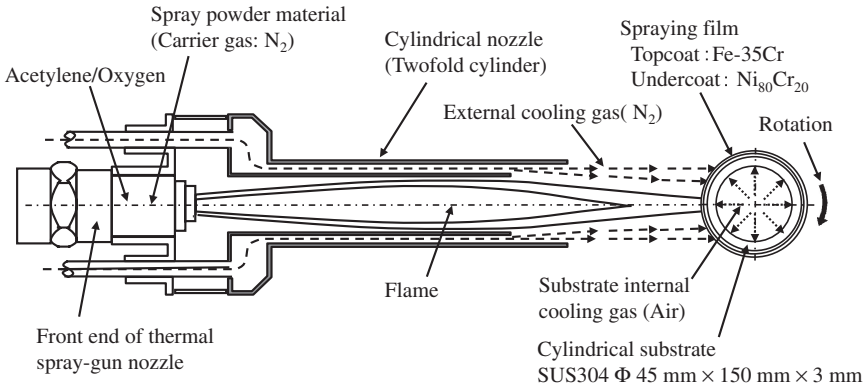

Fig. 1 Schematic illustration of the cylindrical-nozzle type thermal spray gun and the cylindrical substrate that is rotating during the spraying.

Table 1 Thermal spraying condition.

Acetylene	35.4 dm^3/min
Oxygen	35.4 dm^3/min
External cooling gas (N_2)	290 dm^3/min
Substrate internal cooling gas (Air)	0.03 MPa
Gun scan rate	30 mm/s
Substrate rotating speed	220 rpm
Thickness of undercoat layer ($Ni_{80}Cr_{20}$)	300 μm
Thickness of top coat layer (Fe-based amorphous)	500 μm

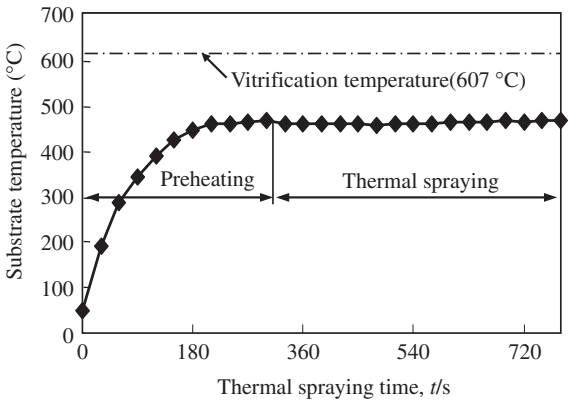

Fig. 2 Relationships between the surface temperatures of the cylindrical substrate as a function of the thermal spraying time with scanning the spray gun.

thermal spraying conditions. In order to keep a reduction atmosphere in the flame, an acetylene-rich gas fuel mixture was used. Nitrogen gas was introduced into the cylindrical nozzle to control the temperatures of the powder particles in the sprayed flame and the substrate and to prevent the formation of oxides in the coating film. To keep the moderate temperature at the surface of the cylindrical substrate, the cooling air was introduced into the internal bore of the substrate. The thermal spray gun was mounted on a robot arm, scanned at the rate of 30 mm/s in feed rate and 220 rpm in rotating speed of the cylindrical substrate. The spraying film consists of two layers; the undercoat layer of $Ni_{80}Cr_{20}$ (at%) alloy on the SUS304 substrate with the thickness of about 300 μm and the top coat layer of the Fe-35Cr amorphous alloys with the thickness of 500 μm.

Figure 2 shows the relationships between the surface temperatures of the cylindrical substrate as a function of the thermal spraying time with scanning the spray gun. Surface temperature at the center point of the cylindrical substrate in the long side was measured by radiation thermometer. The substrate temperature was increased gradually with increasing the spraying time and then saturated to below the vitrification temperature of the Fe-35Cr alloy (607°C).

3. Results

3.1 Structure of the coating films

Figure 3 shows a macroscopic photograph of the Fe-35Cr amorphous coated cylindrical sample (Fig. 3(a)) and a SEM-micrograph of the cross section of the coating film on the SUS304 substrate (Fig. 3(b)). The spraying film consists of two layers. The Fe-35Cr amorphous film with 500 μm thickness was coated on the Ni-Cr layer (300 μm). The surface of the coated cylindrical sample was ground with a diamond grindstone and finished up. As a result, the thickness of the remained Fe-35Cr coating film was about 300 μm. As shown in these figures, high-quality sprayed film without cracking, peeling and inclusion of oxides can be produced.

Figure 4 shows the X-ray diffraction pattern of the Fe-35Cr thermal spray coating film. X-ray diffraction peaks are well-broadened, indicating structure of the film is the amorphous.

Figure 5 shows a TEM image and a selected area diffraction pattern (SADP) of the sprayed Fe-35Cr coating film. It consists of amorphous phase in general. The SADP with halo rings also supports that the coating film has an amorphous structure.

3.2 Corrosion tests

Figure 6 shows SEM micrographs of the Fe-10Cr and the Fe-35Cr amorphous coating films before and after immersion tests for 2 h and 24 h in 35% hydrochloric acid. In the case of the Fe-10Cr coating film, severe corrosion behavior was observed on the surface of the films only after the immersion time of 2 h. On the contrast, corrosion of the Fe-35Cr coating film scarcely progressed after the immersion time of 24 h, indicating the excellent corrosion resistance in the 35% hydrochloric acid.

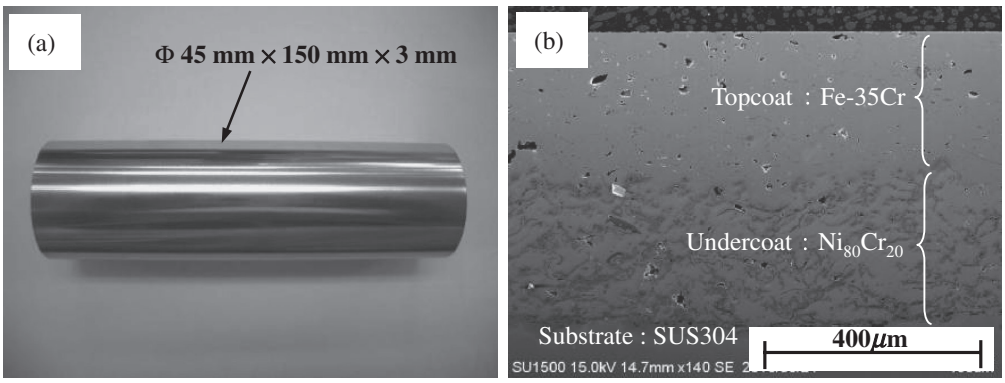

Fig. 3 Macroscopic photograph of the Fe-35Cr amorphous coated cylindrical sample (Fig. 3(a)) and a SEM-micrograph of the cross section of the coating film on the SUS304 substrate (Fig. 3(b)).

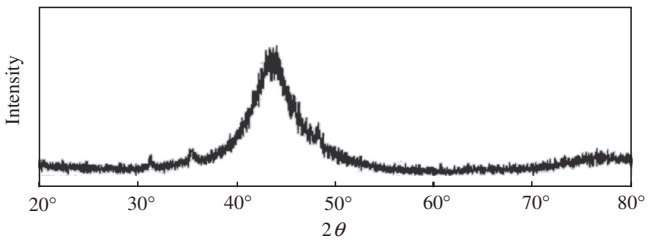

Fig. 4 X-ray diffraction pattern of the Fe-35Cr thermal spray coating film. (CuKα radiation with a graphite monochrometer, 40 KV–20 mA)

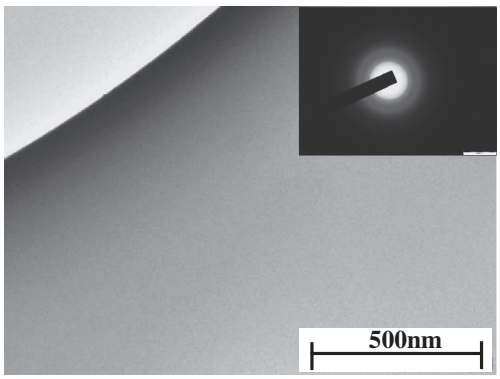

Fig. 5 TEM image and a selected area diffraction pattern (SADP) of the sprayed Fe-35Cr coating film. It consists of amorphous phase in general.

Table 2 shows the weight changes of Fe-10Cr and Fe-35Cr amorphous coating film samples after the corrosion resistance tests. For comparison, some Fe-based amorphous alloy ribbons containing various chromium and molybdenum contents produced by the single roller type melt spinning apparatus were examined for the maximum corrosion immersion time of about 1,008 h. In this case, Fe-10Cr and Fe-35Cr amorphous spray coating films were separated from the substrate, and then immersed in 35% hydrochloric acid for the maximum period of about 24 h.

With increasing the chromium content up to 35 at%, the corrosion weight loss in hydrochloric acid decreased drastically. While, when the chromium content increased to 45 at%, severe brittleness of the sample was observed, and the samples were separated to the small pieces after the immersion test. So, the Fe-based amorphous coating films containing 35 at%-Cr may be the optimal composition for the spray coating layer.

4. Discussion

The internal stress is generated by the difference of the linear expansion coefficients of the coating film and the substrate. Fe-35Cr film is hard and brittle materials, therefore, cracking and peeling are easy to occur on the coating film when the internal stress is generated.

Table 3 shows the linear expansion parameters of the coating films and substrates and expected internal stress of tension or compression in the top coating film. In order to decrease the internal stress, additional temperature control of the substrates may be effective. For example, the linear expansion coefficients of Fe-35Cr top coating film, Hastelloy C substrate and SUS304 substrate are 12.1, 11.9 and 17.4×10^{-6}, respectively. So, heating of the Hastelloy C and cooling of the SUS304 are effective to decrease the internal stress in the top coating film.

Figure 7 shows the schematic illustration of the coating films that consist of the Fe-35Cr top coating film and the $Ni_{80}Cr_{20}$ undercoating film on the SUS304 cylindrical substrate. In this case, we calculated the internal stress in each layers by using a simple flat plates model as schematically shown in Fig. 8. Figure 8(a) shows the condition of just after the thermal spraying at 470°C. The Fe-35Cr top coating film, the $Ni_{80}Cr_{20}$ undercoating film and the SUS304 substrate are assumed to be the same length at 470°C. At this condition, there is no residual stress in each layer. When the temperature is decreased from 470°C to 20°C, the thermal shrinkage can be observed in each layer as shown in Fig. 8(b). In this case, each layer is separated and shrunk independently. Practically, as shown in Fig. 8(c), each layer is strongly connected in each boundary. During cooling from 470°C to 20°C, the length of the substrate may shrink more than that of the sprayed films so that the compression stress is generated in the Fe-35Cr sprayed films.

Table 4 shows the linear expansion coefficients and the young's moduluses of topcoat (Fe-35Cr), undercoat ($Ni_{80}Cr_{20}$) and substrate (SUS304). The linear expansion coefficients of Fe-35Cr were obtained by TMA at the present

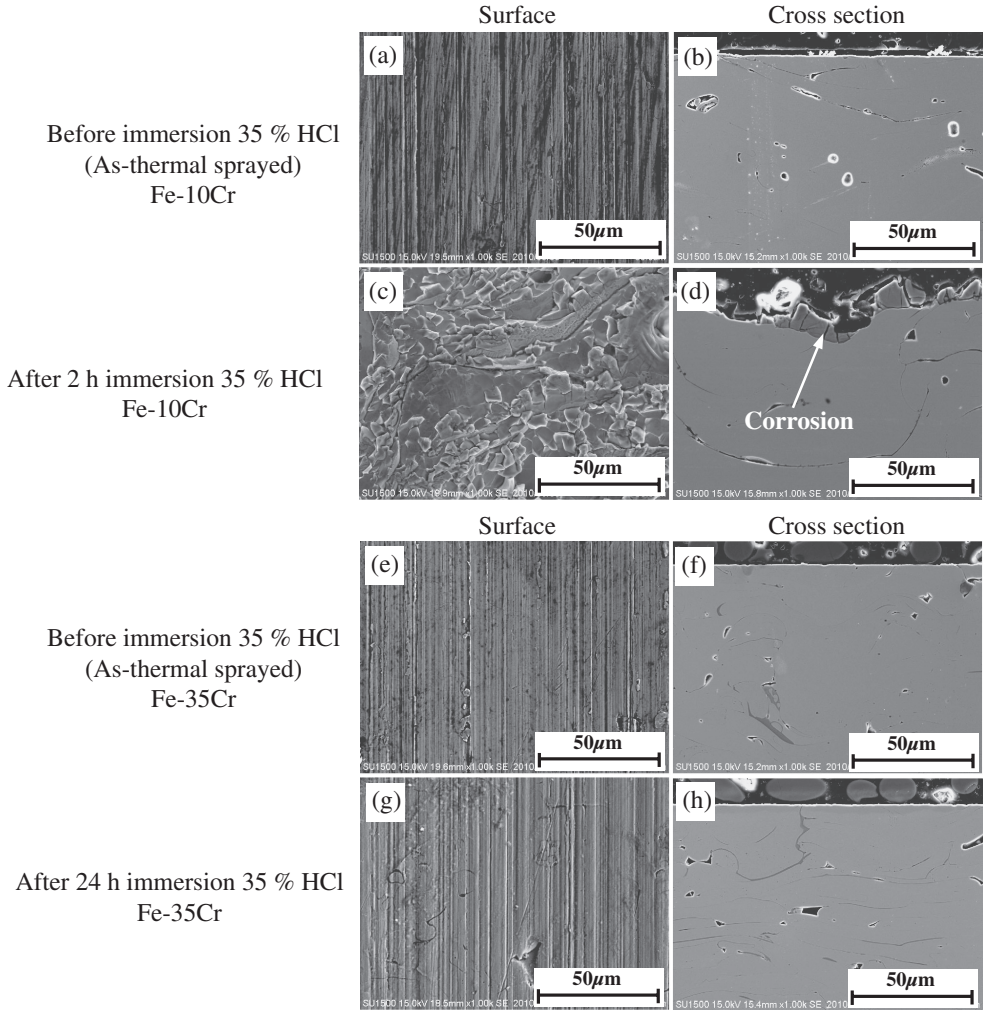

Fig. 6 SEM micrographs of the Fe-10Cr and the Fe-35Cr amorphous coating films before and after immersion tests for 2 h and 24 h in 35% hydrochloric acid.

Table 2 Weight changes of Fe-10Cr and Fe-35Cr amorphous coating film samples after the corrosion resistance tests.

Weight loss (%)

	Item	Fe-45Cr	Fe-35Cr		Fe-25Cr	Fe-16Cr	Fe-10Cr	
		$Fe_{26}Cr_{45}Mo_9P_{13}C_7$	$Fe_{38}Cr_{35}Mo_7P_{13}C_7$		$Fe_{20}Cr_{25}Mo_5Ni_{30}P_{13}C_7$	$Fe_{32}Cr_{16}Mo_2Ni_{30}P_{13}C_7$	$Fe_{70}Cr_{10}P_{13}C_7$	
		Ribbon	Ribbon	Sprayed film	Ribbon	Ribbon	Ribbon	Sprayed film
Corrosive liquids	Hydrochloric acid, 35%	(1008 h)*1	0 (1008 h)	~0 (24 h)	(72 h)*1	(72 h)*1	−100 (6 h)	−20 (2 h)
	Sulfuric acid, 98%*2	0	0	—	0	−0.5	0	—
	Nitric acid, 60%*2	−3.5	0	—	0	−0.6	−5.5	—
	Aqua regia*2	0	−4.7	—	−0.9	—	−19.2	—
	Sodium hypochlorite, 12%*2	−7.8	−1.1	—	+11.0	−1.3	−1.2	—
Hardness (HV)*3		1143	1074	923	888	726	863	708
Ductility		Low	Low	—	Middle	Middle	High	—
Difficulty level of forming		Difficulty	Difficulty	—	Moderate difficulty	Moderate simplicity	Simplicity	—

*1: The samples were separated to the small pieces after the immersion test for several times shown in parentheses.
*2: The amorphous alloy ribbons were examined for the maximum corrosion immersion time of about 1,008 h in these corrosive liquids.
*3: Micro Vickers hardness weight was 50 gf.

Table 3 Linear expansion parameters of the coating films and substrates and expected internal stress of tension or compression in the top coating film.

Materials		Linear expansion coefficient (10^{-6}/°C)	Difference of Linear expansion coefficients* (10^{-6}/°C)	Expected internal stress in the top coating film	Temperature control of substrate
Top coating film (Fe-35Cr)		12.1	0	—	—
Undercoating film ($Ni_{80}Cr_{20}$)		14.3	2.2	Compression	Cooling
Substrate	Hastelloy C	11.9	−0.2	Tension	Heating
	Ti	8.6	−3.5	Tension	Heating
	SUS316	17.5	5.4	Compression	Cooling
	SUS304	17.4	5.3	Compression	Cooling
	SUS403	13.3	1.2	Compression	Cooling
	Fe	10.8	−1.3	Tension	Heating

*Standard is the linear expansion coefficient of the top coating film.

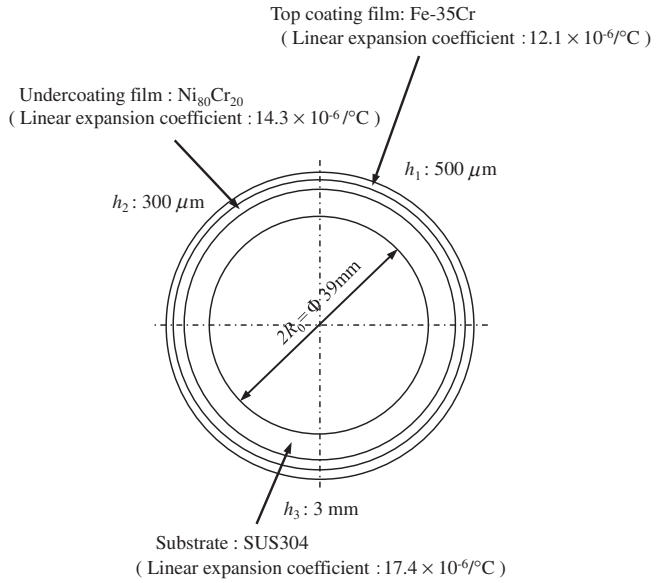

Fig. 7 Schematic illustration of the coating films that consist of the Fe-35Cr top coating film and the $Ni_{80}Cr_{20}$ undercoating film on the SUS304 cylindrical substrate.

study. The linear expansion coefficients and the young's moduluses of $Ni_{80}Cr_{20}$ and SUS304 were referred from Ref. 17). The young's moduluses of Fe-35Cr and $Ni_{80}Cr_{20}$ were assumed to be the same values at the present study.

The residual stress for each layer is derived from the following equations,

1) Balance of the stress,

$$\sigma_1 h_1 + \sigma_2 h_2 + \sigma_3 h_3 = 0, \tag{1}$$

2) Shrinkage allowance,

$$\lambda_1 = \alpha_1 \Delta t_1 L_0 + \frac{\sigma_1 L_0}{E_1},\ \lambda_2 = \alpha_2 \Delta t_2 L_0 + \frac{\sigma_2 L_0}{E_2},$$
$$\lambda_3 = \alpha_3 \Delta t_3 L_0 + \frac{\sigma_3 L_0}{E_3}, \tag{2}$$
$$\lambda_1 = \lambda_2 = \lambda_3, \tag{3}$$

3) Residual stress of top coating film,

$$\sigma_1 = \frac{h_3 E_3(\alpha_3 \Delta t_3 - \alpha_1 \Delta t_1) + h_2 E_2(\alpha_2 \Delta t_2 - \alpha_1 \Delta t_1)}{h_1 + \frac{E_3}{E_1} h_3 + \frac{E_2}{E_1} h_2}, \tag{4}$$

where,

h: Thickness of the layer, E: Young's modulus,
α: Linear expansion coefficient, λ: Shrinkage allowance,
Δt: Quantity of temperature depression, σ: Residual stress,
L_0: Original length, L: Final length,
Index 1: Topcoat, 2: Undercoat, 3: Substrate,
$h_1 = 0.5$ mm, $h_2 = 0.3$ mm, $h_3 = 3.0$ mm,
$\Delta t_1 = -450$°C, $\Delta t_2 = \Delta t_3 \leqq -450$°C.
$\alpha_1 = 12.1 \times 10^{-6}$/°C, $\alpha_2 = 14.3 \times 10^{-6}$/°C, $\alpha_3 = 17.4 \times 10^{-6}$/°C,
$E_1 = E_2 = 66.5$ Gpa, $E_3 = 175.2$ Gpa,

Table 5 shows the calculated residual stress and strain of the Fe-35Cr top coating film with various coating conditions. In the direct coating of the Fe-35Cr film on the SUS304 substrate (Table 5(a)), large compression residual stress and strain were generated in the Fe-35Cr film. With use of the $Ni_{80}Cr_{20}$ undercoating film, residual stress and strain were somewhat decreased from 149 N/mm^2 to 146 N/mm^2 (Table 5(b)). In order to decrease the residual stress and strain, we have proposed the forcibility cooling of the substrate, such as the air-cooling of the substrate during spray coating. As shown in Table 5(c) and (d), when the substrate temperatures were decreased to 314 and 316°C, respectively, the residual stress and strain were decreased to almost zero.

Figure 9 shows the influence of the thickness of $Ni_{80}Cr_{20}$ undercoating film and air-pressure for cooling the SUS304 substrate on quality of the Fe-35Cr top coating film. In order to obtain the good quality Fe-35Cr top coating film, thickness of the $Ni_{80}Cr_{20}$ undercoating film needs more than 350 μm with no air pressure for substrate-cooling. With increasing the air-pressure, necessary thickness of the $Ni_{80}Cr_{20}$ undercoating film decreased linearly to about 250 μm at the air-pressure of 0.03 MPa.

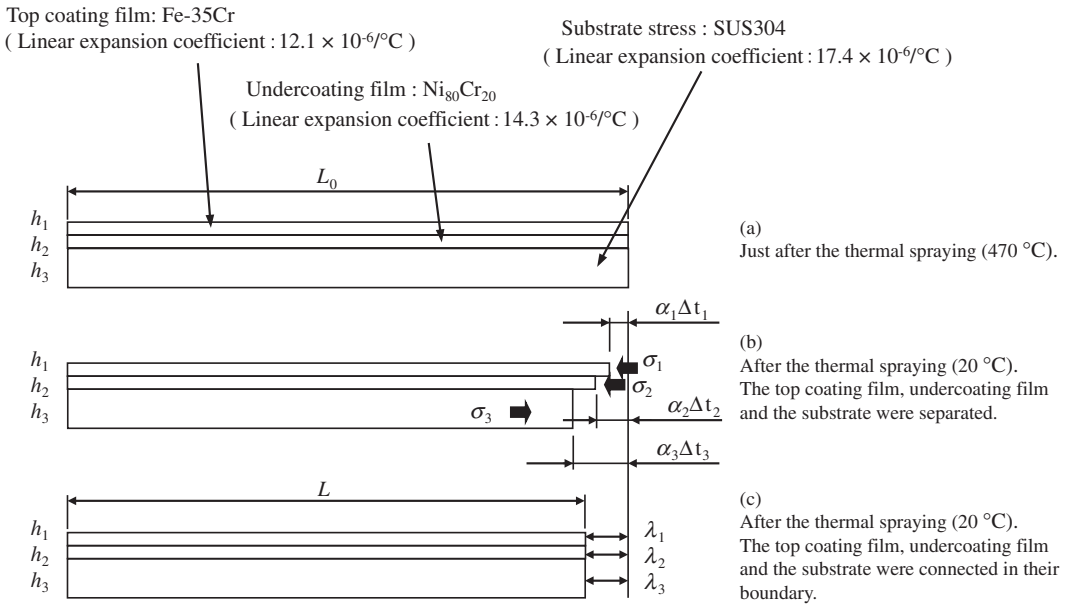

Fig. 8 Internal stress in each layers by using a simple flat plates model as schematically.

Table 4 Linear expansion coefficients and young's moduluses of topcoat (Fe-35Cr), undercoat ($Ni_{80}Cr_{20}$) and substrate (SUS304).

Temperature (°C)	Linear expansion coefficient (10^{-6}/°C)			Young's modulus (GPa)		
	Topcoat (Fe-35Cr)*1	Undercoat ($Ni_{80}Cr_{20}$)*2	Substrate (SUS304)*2	Topcoat (Fe-35Cr)*3	Undercoat ($Ni_{80}Cr_{20}$)*2	Substrate (SUS304)*2
	α_1	α_2	α_3	E_1	E_2	E_3
20	—	13.4	16.4	69.4	69.4	199.8
100	11.4	13.7	16.8	70.1	70.1	189.3
200	13.4	14.1	17.2	69.6	69.6	179.3
300	13.4	14.5	17.6	67.5	67.5	169.8
400	10.8	14.9	18.0	63.9	63.9	160.8
500	11.4	15.3	18.4	58.7	58.7	152.2
Average	12.1	14.3	17.4	66.5	66.5	175.2

*1: The linear expansion coefficients of Fe-35Cr were obtained by TMA at the present study.
*2: The linear expansion coefficients and the young's moduluses of $Ni_{80}Cr_{20}$ and SUS304 were referred from Ref. 17).
*3: The Young's moduluses of Fe-35Cr and $Ni_{80}Cr_{20}$ were assumed to be the same values at the present study.

Table 5 Calculated residual stress and strain of the Fe-35Cr top coating film with various coating conditions.

Calculation condition		Thickness h (mm)			Temperature gradient Δt (°C)		Fe-35Cr		
		Topcoat	Undercoat	Substrate	Topcoat	Substrate	Residual σ (N/mm^2)	Residual ε (%)	λ (%)
(a)	(Fe-35Cr)+(SUS304)	0.50	—	3.00	450	450	−149.16	−0.224	−0.769
(b)	(Fe-35Cr)+($Ni_{80}Cr_{20}$)+(SUS304)	0.50	0.30	3.00	450	450	−146.28	−0.220	−0.764
(c)	(Fe-35Cr)+(Air-SUS304)*	0.50	—	3.00	450	314	−1.16	−0.002	−0.546
(d)	(Fe-35Cr)+($Ni_{80}Cr_{20}$)+(Air-SUS304)*	0.50	0.30	3.00	450	316	−1.10	−0.002	−0.546

*SUS304 substrates are air-cooled during spray coating.

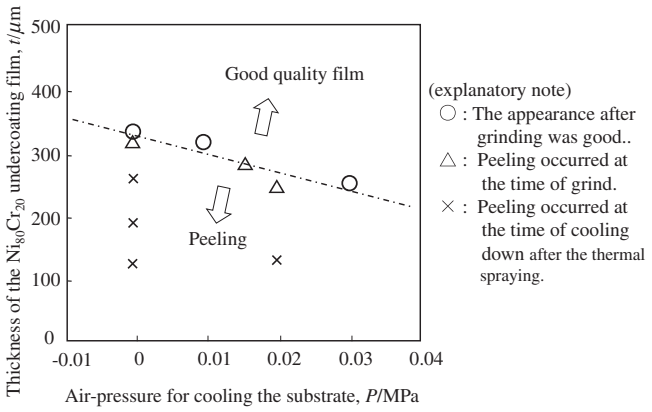

Fig. 9 Influence of the thickness of $Ni_{80}Cr_{20}$ undercoating film and air-pressure for cooling the SUS304 substrate on quality of the Fe-35Cr top coating film.

5. Summary

The Fe-35Cr amorphous coating films having high hardness and high corrosion resistance have been produced by the thermal spraying technique with the cylindrical nozzle on the shaft sleeve shaped cylindrical SUS304 substrates. The internal stress is generated by the difference of the linear expansion coefficients of the coating film and the substrate. Fe-35Cr is hard and brittle materials, therefore, cracking and peeling are easy to occur on the coating film. When the Fe-35Cr top coating film on the SUS304 substrate was used, large internal compression stress was generated on the top coating film. The cooling of the ductile $Ni_{80}Cr_{20}$ undercoating is effectively to decrease the internal stress. Corrosion tests of the sprayed films were also done under the severe immersion conditions of 35% hydrochloric acid. In the case of the Fe-10Cr coating film, severe corrosion behavior was observed on the surface of the films only after the immersion time of 2 h. On the contrast, corrosion of the Fe-35Cr coating film scarcely progressed after the immersion time of 24 h.

REFERENCES

1) A. Kobayashi, S. Yano, H. Kimura and A. Inoue: Surf. Coat. Technol. **202** (2008) 2513.
2) Z. Zhou, L. Wang, F. C. Wang, H. F. Zhang, Y. B. Liu and S. H. Xu: Surf. Coat. Technol. **204** (2009) 563.
3) A. H. Dent, A. J. Horlock, D. G. McCartney and S. J. Harris: Surf. Coat. Technol. **139** (2001) 244.
4) S. Yoon, H. J. Kim and C. Lee: Surf. Coat. Technol. **200** (2006) 6022.
5) M. Naka, K. Hashimoto and T. Masumoto: J. Japan Inst. Metals **38** (1974) 835.
6) K. Hashimoto: J. Japan Inst. Metals **15** (1976) 203.
7) K. Hashimoto: J. Japan Inst. Metals **18** (1979) 362.
8) K. Asami, H. Kimura and A. Inoue: J. Jpn. Soc. Powder Powder Metall. **54** (2007) 795.
9) K. Kishitake, H. Era and F. Otsubo: J. JTSS **5** (1996) 476.
10) F. Otsubo, H. Era and K. Kishitake: Quarterly J. Japan. Weld. Soc. **19** (2001) 54.
11) M. Fukumoto, C. Yokoi, M. Yamada, T. Yasui, M. Sugiyama, M. Ohara and T. Igarashi: Quarterly J. Japan. Weld. Soc. **25** (2007) 323.
12) M. Fukumoto, Y. Okuwa, M. Yamada, T. Yasui, Y. Motoe, K. Nakashima and T. Igarashi: Quarterly J. Japan. Weld. Soc. **26** (2008) 74.
13) N. Nagao, M. Komaki, R. Kurahashi and Y. Harihara: J. Japan Inst. Metals **71** (2007) 742–746.
14) T. Fukushima and S. Kuroda: Quarterly J. Japan. Weld. Soc. **20** (2002) 439.
15) N. Sakakibara, Y. Manabe, Y. Hiromoto and Y. Kobayashi: Quarterly J. Japan. Weld. Soc. **24** (2006) 181.
16) M. Komaki, T. Mimura, Y. Kusumoto, R. Kurahashi, M. Kouzaki and T. Yamasaki: Mater. Trans. **51** (2010) 1581–1585.
17) T. Ishida: Nagasaki University's Academic Output Site, http://hdl.handle.net/10069/6915, (1998).